

A Novel of Repulsive Function on Artificial Potential Field for Robot Path Planning

H. H. Triharminto, O. Wahyunggoro, T. B. Adji, A. I. Cahyadi, and I. Ardiyanto

Electrical Engineering and Information Technology Department, Universitas Gadjah Mada, Yogyakarta, Indonesia

Article Info

Article history:

Received July 27, 2016

Revised

Accepted

Keyword:

APF

Local Minima

GNRON

Potential Function

ABSTRACT

In this paper, the issue of local minima associated with GNRON (Goal Nonreachable with Obstacles Nearby) has been solved on the Artificial Potential Field (APF) for robot path planning. A novel of repulsive potential function is proposed to solve the problem. The consideration of surrounding repulsive forces gives a trigger to escape from the local minima. Addition of logarithmic function on the repulsive force which considers relative distance between the robot and the goal ensures that the goal position is the global optima of the total potential. Simulation conducted to prove that the proposed algorithm can solve GNRON and local minima problem on APF. Scenario of each simulation set in different type of obstacle and goal condition. The results show that the proposed method is able to handle local minima and GNRON problem.

Copyright © 201x Institute of Advanced Engineering and Science.

All rights reserved.

Corresponding Author:

Hendri Himawan Triharminto

Electrical Engineering and Information Technology Department, Universitas Gadjah Mada

Jl. Grafika No. 2 Kampus UGM, Yogyakarta, Indonesia

(+6280274)547506, 510983

kanghimawan@gmail.com

1. INTRODUCTION

A path planner on robot applications plays an important role for fulfilling objective of the robot, such as find out the feasible path starting from the initial and goal position and avoiding collision with obstacles. The process of path planning algorithm can be described as follows: first, start with data environment acquisition, then setup the mission planning, after that develop the path planning, and finally, control the robot based on the generated path planning [1]. Hence, the path planning aims to guide the controller to reach the mission planning.

There are several parameters which has to be considered in the path planning field, e.g. distance, safety, and applicability to the real robot and environments [2]. The distance metric as the measurement means that the path which gives the shortest distance toward a goal will be considered as the optimal path. The safety parameter means the robot must ensure the trajectory toward to the goal is not colliding with the other objects. The applicability relates to application in the real time system which means the algorithm does not generate path that does not fulfilling kinematic constraint. The examples of kinematic constraint are minimum turning radius, maximum linear and angular velocities [3].

Dynamic constraints has two paradigms i.e. the dynamic environment which means the environment that changes dynamically that could be moving obstacle or alteration of the environment while the robot was running [4]. On the other hands, dynamic constraints means the force is used as consideration including mass and dimension. In this paper, for simplicity, the robot is assumed to be a point mass and move in a two dimensional (2-D) workspace. The force of the robot that depends on mass, dimension, inertia are neglected.

1.1. Related Works

Some approaches exist to solve path planning problem. Heuristic search algorithm such as Ant Colony, Particle Swarm Optimization and Artificial Bee Colony were used in term of planning problem [5] [6] [7]. The

weakness of heuristic algorithm is in online path condition which the algorithms are computationally expensive to be pre-planned and it means that the global optimum cannot be achieved easily [8].

Kinematic constraints require feasible and continuous paths. Planning algorithm based on curvature path considers continuous maneuvers, i.e. clothoids arcs, B-spline curves, and Dubin's path [9] [10] [11]. B-spline curve has limitation on the number of control points. Generally, the planning algorithm based on curve merely used on off-line path. One of the example of the curve algorithm for the dynamic environment was proposed by Triharminto et. al. [12].

One of the well-known path planning algorithm is Artificial Potential Field (APF). APF is a planning algorithm that is designed as reactive path for obstacle avoidance. Therefore, the APF is suitable to use for offline and online path generation. The basic concept of APF follows the natural characteristic of electrostatic potential which in the case robot of path planning, the goal position becomes the lowest while initial position is the representative of the highest potential [13]. Consequently, the potential energy will move from the highest to the lowest following the nature of potential field. For avoiding collision with the obstacle, the obstacle is set as opposite direction force that refuses the robot from the obstacles. The APF method is particularly attractive because its effectiveness as real time obstacle avoidance beside its mathematical elegance and simplicity [14]. However, the APF has a problem based on mathematical analysis that is trap situations due to local minima [15] [16]. Additionally, GNRON problem is close correlation with local minima problem [17].

Some researchers tried to solve local minima but the algorithms usually do not consider GNRON problem [18] [19] [20] [21]. All of the proposed algorithms used APF blended with evolutionary algorithm to navigate in an autonomous form without being trapped in local minima. Lei et al. (2010) solved local minima method based on gravity chain that connects initial and goal points [22]. The gravity chain has a role to guide the robot. The other solution handle the local minima on APF is by using harmonic potential [23] [24]. This local minima problem is solved by forcing local potential extrema to lie on the boundaries of obstacles through the use of harmonic potentials, that is, of potential functions V satisfying Laplaces equation, $\nabla^2 V = 0$. Disadvantage of these methods is that Laplaces equation has to be solved numerically over the whole state space and it raises the difficulty to find solutions in real-time for dynamic environments [25]. Stream function is used to determined the path without local minima and GNRON problem [28] [29]. Similar to harmonic potential field, Laplace's equation has to be solved in the stream function which means that the algorithm computationally expensive.

The solution proposed eliminating the local minima problem by defining the obstacles potential with exponential function is proposed by Sfeir et al. [30]. Thus, the potential is inactive except when the robot is very close to the goal. The essential structure of potential field is also modified which the total force is null when the robots at the goal point in term of GNRON problem. In the research, the issue that would be interest is the choice of gain parameters. The value of parameters is selected by trial and error. The addition of force implemented to handle local minima [27]. The total force will drag the robot to escape from the local minima. Another weakness appears when the distance between the robot and the goal equals to the distance between the robot and the obstacle. Merging between APF and evolutionary algorithm is one of the solution to handle the problems in APF including determination of gain parameter [26]. Mei et. al. (2013) used hybrid algorithm APF and Bug algorithm [31]. The bug algorithm was used to escape from GNRON and local minima [32]. Hybrid algorithm switches from APF to evolutionary algorithm and the trade-off is cost of computational complexity.

This paper proposed an adhoc solution to solve the GNRON and local minima problems in APF. Therefore, this paper has a contribution to develop a new potential field function to cope both local minima and GNRON problem. The organization of this paper is as follows. Section 2 explains the APF and the existing both of local minima and GNRON problem, the third section describes the new repulsive function and how to cope both of the problems. And finally, the last two sections deliver simulation result, discussion, and the rest is the conclusion of the research with possible future work.

2. LOCAL MINIMA AND GNRON PHENOMENA

As in the explanations, the APF has two different potential functions [33]. Let the position of the robot in the workspace is denoted by $q = [x \ y]^T$, the most commonly attractive force of APF [14] can be modeled as

$$F_{att}(q) = -\nabla V_{att}(q), \quad (1)$$

where

$$V_{att}(q) = \frac{1}{2} \xi \rho^2(q, q_{goal}). \quad (2)$$

Variable ξ is an attractive gain parameter which has positive value and $\rho(q, q_{goal}) = \|q_{goal} - q\|$ is the distance between robot (q) in certain position and the goal point (q_{goal}). From the mathematical formulation, it can be seen

that the attractive force converges linearly toward zero as the robot approaches the goal. That characteristic will be applicable for control system which means it will not harm the actuator of the robot.

The other potential function is in the obstacle which the formula for a single point obstacle is

$$F_{rep}(q) = \nabla V_{rep}(q), \quad (3)$$

where

$$V_{rep}(q) = \begin{cases} \frac{\eta}{\sqrt{\rho(q, q_{obs})}}, & \text{if } \rho(q, q_{obs}) \leq \rho_o \\ 0, & \text{if } \rho(q, q_{obs}) > \rho_o \end{cases} \quad (4)$$

Variable η is a repulsive gain parameter and $\rho(q, q_{obs})$ is the distance between the robot and the obstacle position and ρ_o is a positive constant denoting the c-obstacle of robot dimension.

From the repulsive and attractive force, the total of the force field can be determined as sum of attractive and repulsive force

$$F_{total} = F_{att} + F_{rep}. \quad (5)$$

The total force represents path of robot.

2.1. Local Minima

According to the used force, the essential problem of the APF is the trap in local minima. The problem can be found when $F_{total} = 0$. For instance, when the robot initial position, $q = [a \ 0]^T$, for some positive number a collinear with the goal, $q_{goal} = [a \ 11]^T$ as shown in Fig. 2. In between the robot and the obstacle, there are two obstacles in $q_{obs} = [8 \ 10]^T$ and $q_{obs} = [10 \ 10]^T$ respectively. Thus, F_{att} in the x axis can be computed equal to 0 if $\{\forall \xi > 0\}$. Assuming that $\eta = 1$, it is clear that the $F_{att} = 1$ for $q_{obs} = [10 \ 10]^T$ and $F_{att} = -1$ for $q_{obs} = [10 \ 10]^T$. Consequently, in the x axis, $F_{rep} = 0$, although $\{\forall \eta > 0\}$. Let focus on y axis, if the robot moves toward goal point, for instance, now, the robot is at $q = [9 \ 9]^T$ which means the value of $\rho(q, q_{obs}) = 1$. Then, value of $F_{rep} = 1$ for both of the obstacle and the total of $F_{rep} = 2$ in a positive value.

The condition of local minima is met when the attractive gain parameter has been set of 1 which means $F_{att} = -2$ in a negative value due to the negative gradient of the attractive potential. Therefore, the total force (F_{total}) based on (5) will be 0 as illustrated in Fig. 1. From the Fig. 1, it shows that the robot trap at $q = [9 \ 4]$ which $F_{total} \approx 0$ and cannot reach the goal. The robot assumes that the local minima is as the global optimum.

It has be noted that, in that case with assumption that the dimension of the robot is 1 unit square in the workspace, it is obviously that the alteration value of attractive and repulsive will yield two conditions, i.e. the robot will hit the obstacle or the robot will meet local minima. To escape the local minima, external force has to be proposed that will be explained in Section 3.

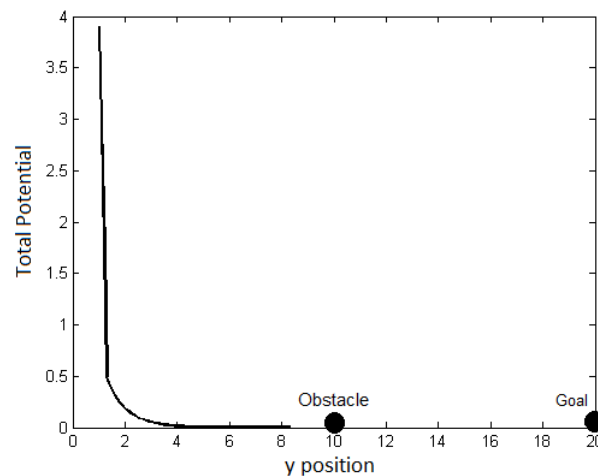


Figure 1. Total potential function with respect to y axis in local minima problem

2.2. GNRON

The GNRON problem is part of local minima problem. This problem exists when the goal is very close to the obstacle. For example, consider the scenario is almost similar to local minima as in the aforementioned but the goal point is set of $q_{goal} = [9 \ 8]^T$ as in Fig. 2. If the robot is moving along y axis and reaching the goal, then $F_{att} = 0$ for the x and y axes. On the repulsive force, similar to local minima in the x axis, $F_{rep} = 0$ while in the y axis, total of repulsive force of both obstacle is $F_{rep} = -2$. Based on the rules (4) and (5), at $q = [9 \ 8]^T$, the corresponding repulsive is given by $\rho(q, q_{obs}) \leq \rho_o$. Then, even though the robot should reach the goal but it is repulsed away by the repulsive force. The strategy of this problem is set the repulsive force equal to 0 when the robot reach the goal as in Section 3.

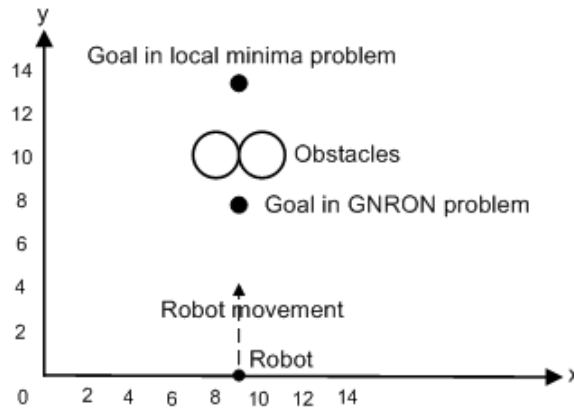


Figure 2. Location of the robot, goal in local minima and GNRON problem, and Obstacle in a 2-D case

3. NEW REPULSIVE POTENTIAL FUNCTIONS

3.1. Repulsive Function for Local Minima Problem

The local minima problem arises because the total force of potential field equals to 0. The problem will make the robot does not move or in static condition due to insufficient force. As mentioned before, external force is a solution to escape from the local minima. It has to be considered that the external force in attractive force is not possible due to the global optimum is met when $F_{att} = 0$. Thus, addition of force in the attractive will make the robot does not meet the goal. Alternatively, external force is applied in the repulsive force. The motivation is to construct a new repulsive potential function as

$$V_{rep}(q) = \begin{cases} \frac{\eta}{\sqrt{\rho(q, q_{obs})}} + \psi(q, \zeta), & \text{if } \rho(q, q_{obs}) \leq \rho_o \\ 0, & \text{if } \rho(q, q_{obs}) > \rho_o \end{cases} \quad (6)$$

In comparison with (4), the introduction of

$$\psi(q + \zeta) = \frac{\eta}{\sqrt{\rho((q + \zeta), (q + \zeta)_{obs})}}, \quad (7)$$

ensures that the external force takes the robot escape from local minima. As comparison, the total force from the original potential function and the total force of the new potential function can be seen in Fig. 3a and 3b. Fig. 3a shows the total force in the original scenario without an external force. Fig 3b shows the total potential at the local minima is not equal to 0 because of the addition of $\psi(q + \zeta)$. It is seen by the total force is bigger than the original one and moves to the other place.

The repulsive potential function $F_{rep}(q)$ should have the property that the sum of repulsive force and external force pushes the robot away from the local minima. Since $F_{att} = 0$ and $F_{rep} = 0$, the parameter ζ has to be set properly in order to drag the robot escape from local minima. Let set that F_{min} i. e., the minimum force to move the robot when the robot trapped in the local minima,

$$F_{min} = \psi(q + \zeta) = \sqrt{\psi^2(q_{x+\zeta}) + \psi^2(q_{y+\zeta})}, \quad (8)$$

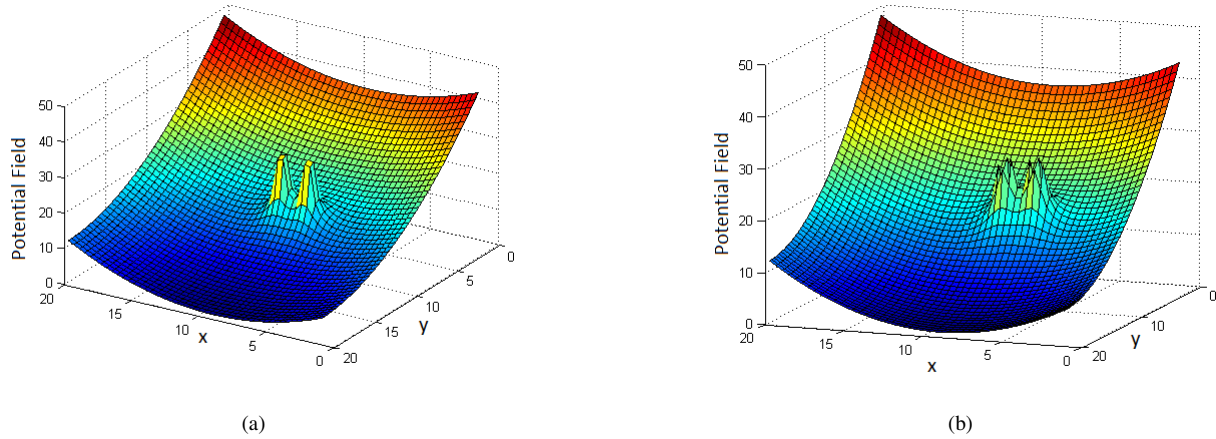


Figure 3. Total potential when (a) the local minima exist (b) the local minima moving from the original place

$\psi(q_{x+\zeta})$ and $\psi(q_{y+\zeta})$ is denoted as repulsive force in the position $(x + \zeta)$ and $(y + \zeta)$ respectively. Defining c_{obs} is the safety distance between the robot and the obstacle that consist of q_x and q_y as

$$c_{obs}^2 = q_x^2 + q_y^2. \quad (9)$$

For simplicity, let assumes that $q_x = q_y = \varsigma$. Then, gradient of $(\partial V_{rep}(q + \zeta)/\partial x, \partial V_{rep}(q + \zeta)/\partial y)$ are

$$\psi^2(q_{x+\zeta}) = \frac{\eta\varsigma}{((\varsigma + \zeta)^2 + \varsigma^2)^{3/2}}, \quad (10)$$

$$\psi^2(q_{y+\zeta}) = \frac{\eta\varsigma}{(\varsigma^2 + (\varsigma + \zeta)^2)^{3/2}}. \quad (11)$$

Substituting (12) and (13) puts into (10) leads to

$$F_{min}^2 = 2 \frac{\eta\varsigma}{(2\varsigma^2 + 2\varsigma\zeta + \zeta^2)^{3/2}}. \quad (12)$$

Let simplifies right hand and left hand side by power $(2/3)$,

$$F_{min}^{4/3} = 2^{(2/3)} \frac{(\eta\varsigma)^{2/3}}{(2\varsigma^2 + 2\varsigma\zeta + \zeta^2)}. \quad (13)$$

Therefore, ζ can be computed as follows.

$$2\varsigma^2 \frac{F_{min}^{4/3}}{2^{(2/3)}(\eta\varsigma)^{2/3}} + 2\varsigma \frac{F_{min}^{4/3}}{2^{(2/3)}(\eta\varsigma)^{2/3}}\zeta + \frac{F_{min}^{4/3}}{2^{(2/3)}(\eta\varsigma)^{2/3}}\zeta^2 = 0, \quad (14)$$

$$\zeta = \frac{-2\varsigma c \pm \sqrt{4\varsigma^2 c^2 - 8\varsigma^2 c^2}}{2c}, \quad (15)$$

where

$$c = \frac{F_{min}^{4/3}}{2^{(2/3)}(\eta\varsigma)^{2/3}} \text{ and } \varsigma = \frac{c_{obs}}{\sqrt{2}}. \quad (16)$$

From (17), there are two solutions of ζ which means the tendentious of robot turning. For example in the Fig. 1, positive value will take the robot takes right turning an negative value will take the robot chooses left turning.

The new potential field for local minima problem will take as a basic potential field for the GNRON problem. It means that the function must be considered and remained the result for local minima problem. The extended potential function for the GNRON problem will be explained below.

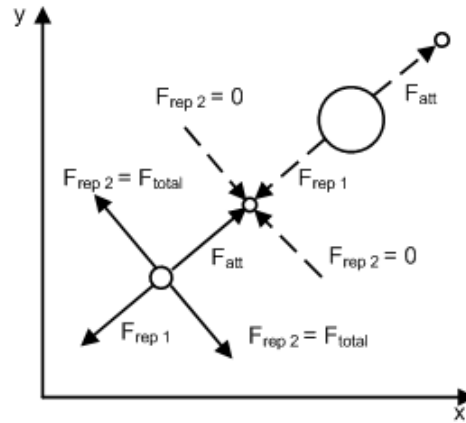


Figure 4. Total force derived by the new potential function

3.2. Repulsive Function for GNRON Problem

The GNRON problem occurs because the total force of potential field in the goal is not zero in consequence of the repulsive force. The distance influences repulsive force due to the fact as the robot approaches the goal, the repulsive potential increases as well. There are several things that have to be considered in the GNRON problem as described as follows.

1. Regarding to local minima problem, the addition function in the GNRON problem has not to be influenced significantly in the computation with the repulsive function in the local minima problem. Consequently, extended function has to be set properly.
2. Some parameters that can be used in order to construct the extended of potential function are $\rho(q, q_{obs})$, $\rho(q, q_{goal})$, and $\rho(q_{obs}, q_{goal})$. It has to be noted that involving the q_{obs} is not applicable in the real time platform due the fact that there are no way (sensor) which is able to detect infinite distance of an obstacle. Consequently, $\rho(q, q_{obs})$ and $\rho(q_{obs}, q_{goal})$ are neglected and it merely uses $\rho(q, q_{goal})$.
3. GNRON problem arises at location which is based on the rule on (4) and it can be said the goal is in the border area between rule on (4) and (5). Thus, in that location, it is obvious $F_{att} = 0$ since $\rho(q, q_{goal}) = 0$ but in contrast, $F_{rep} \neq 0$. Thus, the solution is to make the $F_{rep} = 0$.

Based on the things as in the aforementioned, its motivate to develop new repulsive potential function as

$$V_{rep}(q) = \begin{cases} \frac{\eta \operatorname{sgn}(\rho(q, q_{goal}))}{\sqrt{\rho(q, q_{obs})}} + \frac{\eta \operatorname{sgn}(\rho(q, q_{goal}))}{\sqrt{\rho((q + \zeta), (q + \zeta)_{obs})}}, & \text{if } \rho(q, q_{obs}) \leq \rho_o \\ 0, & \text{if } \rho(q, q_{obs}) > \rho_o \end{cases} \quad (17)$$

where

$$\operatorname{sgn}(\rho(q, q_{goal})) \begin{cases} 1 & \text{if } \rho(q, q_{goal}) \neq 0 \\ 0 & \text{if } \rho(q, q_{goal}) = 0. \end{cases} \quad (18)$$

On (19) and (20), the signum function is used to solve GNRON problem whenever $\rho(q, q_{goal}) \neq 0$ then $F_{rep} \neq 0$ and $\rho(q, q_{goal}) = 0$ then $F_{rep} = 0$. With the $F_{rep} = 0$ at the goal position, it means that the robot has no force when meets the goal and finds the global optimum.

In order to illustrate the total force for both local minima and GNRON problem using the new potential function, Fig. 4 is utilized to explain the applied force in the new potential function. From the Fig. 4, in the local minima problem, $F_{att} = F_{rep1}$ and the additional function generates a new repulsive force F_{rep2} . Thus, in the local minima problem, $F_{total} = F_{rep2}$. On the other hands, in the GNRON problem, the logarithmic function yield $\log 1 = 0$, then force of F_{rep1} and F_{rep2} will be disappear or equal to 0. From the Fig. 4, it is proven that the new repulsive potential field can handle local minima and GNRON Problems.

3.3. Convergence analysis

The total force of potential field is as mentioned on (6). Substituting (19) into (6) leads to

$$\begin{aligned}
 F_{total}(q) &= -\nabla V_{att}(q) + \nabla V_{rep}(q) \\
 &= -\xi \rho(q, q_{goal}) + \frac{\eta \operatorname{sgn}(\rho(q, q_{goal})) \rho(q, q_{obs})'}{\rho(q, q_{obs})^{3/2}} + \\
 &\quad \frac{\eta \operatorname{sgn}(\rho(q, q_{goal})) \rho((q + \zeta), (q + \zeta)_{obs})'}{\rho((q + \zeta), (q + \zeta)_{obs})^{3/2}}.
 \end{aligned} \tag{19}$$

From (21), there are two values of $\operatorname{sgn}(\rho(q, q_{goal}))$, i.e. 0 and 1. If the value is 0, then the repulsive force will be 0. When $F_{rep} = 0$, it is obviously that the system is stable remaining $\rho(q, q_{goal}) = 0$ which affect to $F_{att} = 0$. Consequently, $F_{total} = 0$ while the robot reaches the final point.

Let assumes that $\log\left(\frac{\rho(q, q_{goal})}{\rho} + 1\right) = 1$ for simplicity, equation (27) will be

$$\begin{aligned}
 F_{total}(q) &= -\nabla V_{att}(q) + \nabla V_{rep}(q) \\
 &= -\xi \rho(q, q_{goal}) + \frac{\eta \vec{\rho}(q, q_{obs})'}{c_{obs}} + \\
 &\quad \frac{\eta \rho((q + \zeta), (q + \zeta)_{obs})'}{\rho((q + \zeta), (q + \zeta)_{obs})^{3/2}},
 \end{aligned} \tag{20}$$

remains that the robot position against the obstacle is $\rho(q, q_{obs}) = c_{obs}$ and $c_{obs} > 0$.

As $\rho((q + \zeta), (q + \zeta)_{obs}) = \|q_{obs}(q + \zeta)\| > 0$ (always positive value), it can be replaced with variable that coined as ν , where $\nu > 0$. Then, (28) can be simplified as

$$\begin{aligned}
 F_{total}(q) &= -\nabla V_{att}(q) + \nabla V_{rep}(q) \\
 &= -\xi \rho(q, q_{goal}) + \frac{\eta \vec{\rho}(q, q_{obs})'}{\nu} + \\
 &\quad \frac{\eta \rho((q + \zeta), (q + \zeta)_{obs})'}{\nu}.
 \end{aligned} \tag{21}$$

Now, (21) can be elaborated into state function in two dimensional (x and y), i.e. $F_{total}(x, t)$ and $F_{total}(y, t)$. If it assumes that $F_{total}(x) = \dot{x}$ and $F_{total}(y) = \dot{y}$, then (21) is

$$\begin{aligned}
 \dot{x} &= -\xi(x - x_T) + \frac{\eta(x - x_o)}{c_{obs}} + \frac{\eta(x \pm \zeta - x_o)}{\nu} \\
 \dot{y} &= -\xi(y - y_T) + \frac{\eta(y - y_o)}{c_{obs}} + \frac{\eta(y \pm \zeta - y_o)}{\nu},
 \end{aligned} \tag{22}$$

where (x_o, y_o) is obstacle's position and (x_T, y_T) is goal position or origin point. Since c_{obs} and ν are always positive, then it can be neglected and is assumed equal to 1. Position (0,0) is set as goal position for simplicity. Thus, 22 is modified

$$\dot{x} = -\xi x + \eta(x - x_o) + \eta(x \pm \zeta - x_o). \tag{23}$$

Dividing left and right hands with x , (23) becomes

$$\frac{\dot{x}}{x} = -\xi + 2\eta - \frac{2\eta x_o \pm \eta \zeta}{x}, \tag{24}$$

or in another form

$$\frac{dx}{x} = -\xi + 2\eta - \frac{2\eta x_o \pm \eta \zeta}{x} dt. \tag{25}$$

by integrating left and right hands,

$$\begin{aligned}
 \int \frac{dx}{x} &= \int -\xi + 2\eta - \frac{2\eta x_o \pm \eta \zeta}{x} dt \\
 \ln(x) &= (-\xi + 2\eta - \frac{2\eta x_o \pm \eta \zeta}{x})t.
 \end{aligned} \tag{26}$$

In order to obtain explicit form, exponential function applies on the left and right hands,

$$\begin{aligned} \int \frac{dx}{x} &= \int -\xi + 2\eta - \frac{2\eta x_o \pm \eta \zeta}{x} dt \\ e^{\ln(x)} &= e^{(-\xi + 2\eta - \frac{2\eta x_o \pm \eta \zeta}{x})t} \end{aligned} \quad (27)$$

Therefore, the function x in the time domain

$$\begin{aligned} x(t) &= e^{(-\xi + 2\eta - \frac{2\eta x_o \pm \eta \zeta}{x})t} \\ x(t) &= e^{-(\xi - 2\eta)t} \cdot e^{-\frac{2\eta x_o \pm \eta \zeta}{x}t} \end{aligned} \quad (28)$$

With the same process of \dot{x} , \dot{y} is obtained

$$\begin{aligned} y(t) &= e^{(-\xi + 2\eta - \frac{2\eta y_o \pm \eta \zeta}{y})t} \\ y(t) &= e^{-(\xi - 2\eta)t} \cdot e^{-\frac{2\eta y_o \pm \eta \zeta}{y}t} \end{aligned} \quad (29)$$

Equation (28) and (29) are exponential function which means that a gradient function. Convergent system is acquired by defining

$$\begin{aligned} \xi - 2\eta &> 0 \\ \xi &> 2\eta, \end{aligned} \quad (30)$$

Based on conditions of ζ , if ζ are positive, then

$$\begin{aligned} \frac{\eta(2x_o + \zeta)}{x} &> 0 \\ 2x_o &> -\zeta \end{aligned} \quad (31)$$

and if ζ are negative, then

$$\begin{aligned} \frac{\eta(2x_o - \zeta)}{x} &> 0 \\ 2x_o &> \zeta \end{aligned} \quad (32)$$

. For \dot{y} , (31) becomes

$$\begin{aligned} \frac{\eta(2y_o - \zeta)}{y} &> 0 \\ 2y_o &> \zeta \end{aligned} \quad (33)$$

and

$$\begin{aligned} \frac{\eta(2y_o + \zeta)}{y} &> 0 \\ 2y_o &> -\zeta. \end{aligned} \quad (34)$$

It can be concluded that satisfying (30) until (34) will make a curve response of the system which monotonically to zero. Thus, the system is asymptotically convergent.

4. RESULT AND DISCUSSION

In order to prove performance of the proposed algorithm, the test conducted in the loop simulation. The simulations are divided into the scenario. The first scenario has been proven for local minima problem, the second scenario has been shown how the algorithm handles the GNRON problem, and the last scenario checked the robustness of the algorithm by using a random position for initial, goal, and obstacles.

4.1. Scenario 1

The first experiment is application of the original APF that can be seen in Figure 5a. Parameter ξ and η are 0.2 and 5 respectively. Figure 5a shows that the robot is stuck when it trap in the local minima. The robot cannot move since the $F_{total} = 0$. In the scenario, the robot assumed as a point mass and the safety area (c_{obs}) is set of 2 unit. The application of proposed F_{rep} for local minima can be depicted as in Fig. 5b.

Figure 5b shows the simulation result where the robot can escape from the local minima. The proposed repulsive function drives the robot to the goal while avoiding the obstacles. One of the drawback of proposed method is that oscillation phenomena still occurred that can be seen in Figure 5b. The second thing is that the result path is not the shortest since turning radius of the robot is far away from the c_{obs} .

4.2. Scenario 2

The other scenario was conducted regarding to GNRON problem. For simplicity, the obstacle was reduced into 1 obstacle at (9,10) as illustrated in Fig. 6a. Figure 6a is the example of GNRON phenomena that the global optimum (goal point) is not reachable due to repulsive force. It means that $F_{total} = F_{rep}$ when the robot at the goal and the robot has been repulsed away from the goal. Equation (19) has been implemented to handle GNRON problem that can be seen in Fig. 6b. From Fig. 6b, it can be concluded that the proposed potential function solves the GNRON problem.

4.3. Scenario 3

In this scenario, the obstacles was set randomly in the unstructured shape. The obstacle itself was constructed by several points and represented three objects in the real scenario. The initial and goal point were also set randomly. The results can be seen in the Fig. 7a and 7b.

The red dots is the points that generates the obstacles. The green dots are the safety area (c_{obs}) of an obstacle which set of 1 unit. Formerly, the points is shaping into convex hull. The hull is then adding with virtual points to form the points as an obstacle. Figure 7a and 7b prove the robustness of the algorithm in the different scenario. In the

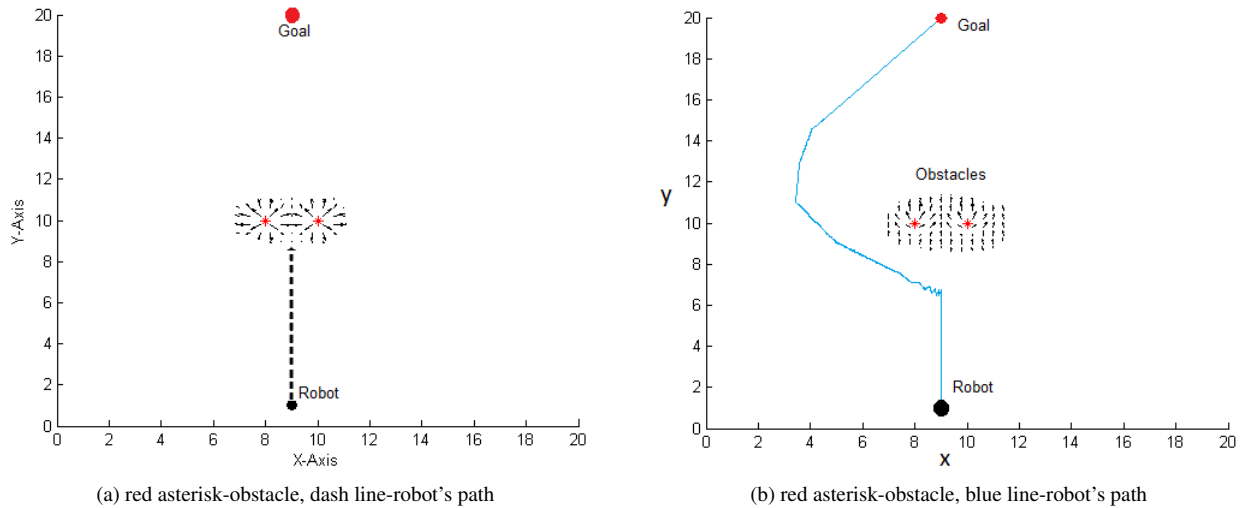


Figure 5. (a) Example of Local Minima Phenomena (b) Result of proposed F_{rep} of Local Minima Phenomena

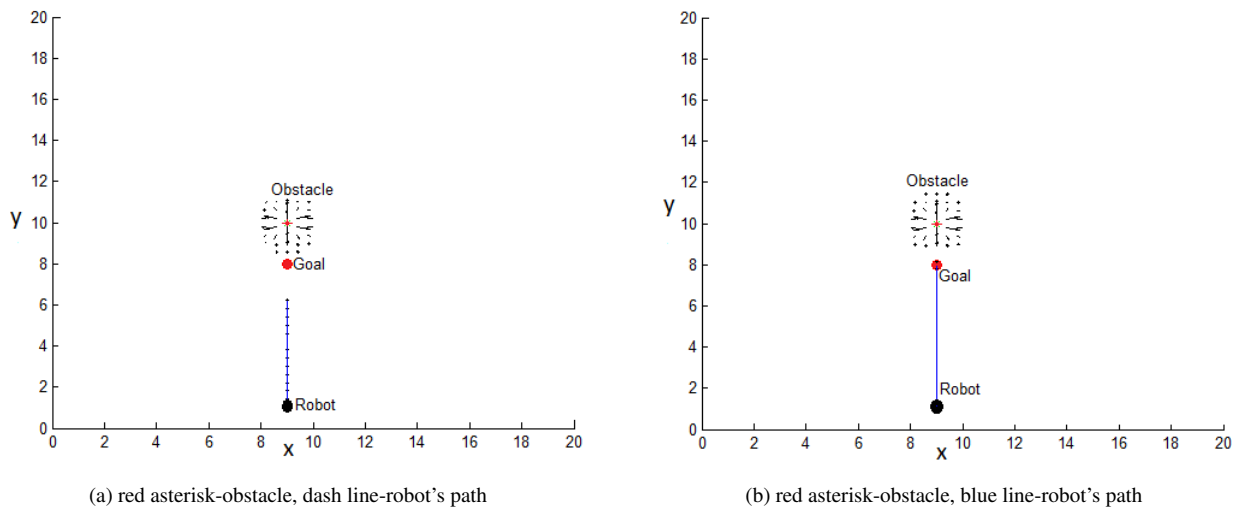


Figure 6. (a) Example of GNRON Phenomena (b) Result of proposed F_{rep} of GNRON

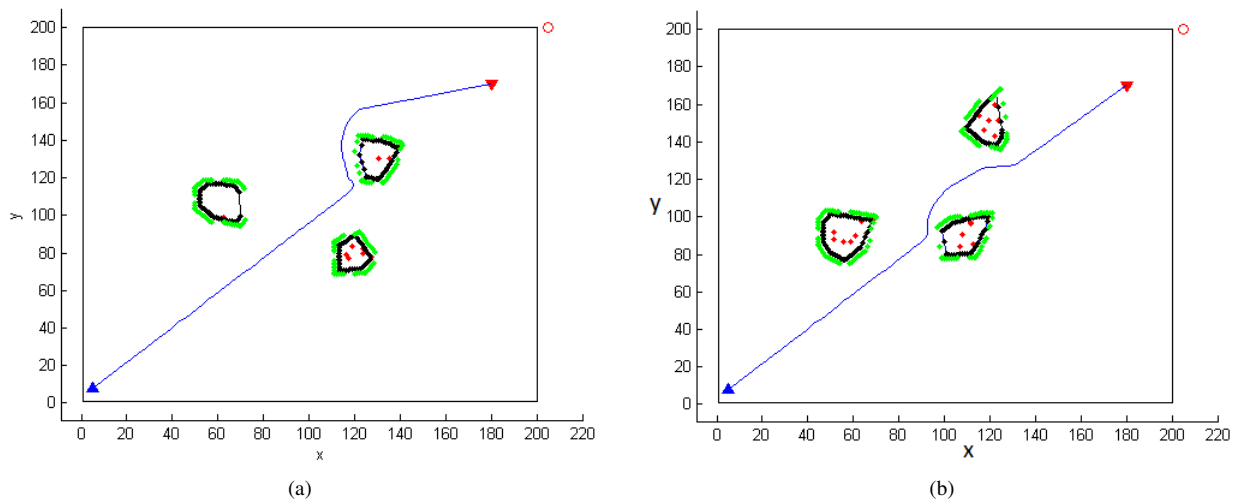


Figure 7. The example results of the proposed method with unstructured obstacles

scenario, the robot can avoid the obstacles successfully. The new repulsive function does not degrading the ability of APF as obstacle avoidance algorithm.

4.4. Discussion

Although the proposed method assures that the robot can handle local minim and GNRON problem with the analytic solution, but it has to be proven that the method is applicable in the real time system. On the other hands, oscillation still occurs in the path generation and it cannot be neglected in the real time system. Thus, implementation of proposed method which considers kinematic and dynamic constraints is the next step for further research.

5. CONCLUSION

This paper has been presented the problem associated with artificial potential field, i.e local minima and GNRON. A new repulsive potential function has been proposed to cope the local minima problem by considering the repulsive function surrounding the robot. The signum function that contains relative distance between the robot and the goal is the proposed addition function in the repulsive field. The repulsive function surrounding the robot will used as the trigger to escape from the local minima and the relative distance will ensure the goal position is the global minimum of the potential function. Simulation results have been verified that the proposed algorithm can solve local minima and GNRON problems.

REFERENCES

- [1] T. Tomic, K. Schmid, P. Lutz, A. Domel, M. Kassecker, E. Mair, I. Grix, F. Ruess, M. Suppa, D. Burschka, "Toward a fully autonomous UAV: Research platform for indoor and outdoor urban search and rescue," *IEEE Robotic Automation Magazine*, vol. 19(3), pp. 46-56, 2012.
- [2] I. Ardiyanto, J. Miura, "Real-time navigation using randomized kinodynamic planning with arrival time field," *Robotics and Autonomous Systems*, vol. 60, pp. 1579-1591, 2012.
- [3] M. Shanmugavel, A. Tsourdos, B. White, R. Zbikowski, "Co-operative path planning of multiple UAVs using Dubins paths with clothoid arcs," *Control Engineering Practice*, vol. 18(9), pp. 1084-1092, 2010.
- [4] H. H. Triharminto, A. S. Prabuwno, T. B. Adj, and N. A. Setiawan, "Adaptive Dynamic Path Planning Algorithm for Interception of a Moving Target," *International Journal Mobile Computing Multimedia Communication*, vol. 5(3), pp. 19-33, 2013.
- [5] S. Chakraborty, "Ant Colony System: An Improved Approach for Robot Path Planning," *International Journal of Hybrid Information Technology*, vol. 7(2), pp. 249-268, 2014.
- [6] J. H. Liang and C.H. Lee, "Efficient collision-free path-planning of multiple mobile robots system using efficient artificial bee colony algorithm," *Advances in Engineering Software*, vol. 79, pp. 47-56, 2015.

- [7] J. Karimi and S. H. Pourtakdoust, "Optimal maneuver-based motion planning over terrain and threats using a dynamic hybrid PSO algorithm," *Aerospace Science and Technology*, vol. 26(1), pp. 60-71, 2013.
- [8] P. Raja and S. Pugazhenth, "Optimal path planning of mobile robots: A review," *International Journal of the Physical Sciences*, vol. 7, no. 9, pp. 1314-1320, 2012.
- [9] M. Elbanhawi, M. Simic, R. N. Jazar, "Continuous Path Smoothing for Car-Like Robots Using B-Spline Curves," *Journal of Intelligent and Robotic System*, vol. 80, pp. 23-56, 2015.
- [10] D. Sabelhaus, F. Roben, L.P. Meyer zu Helligen, P. Schulze Lammers, "Using continuous-curvature paths to generate feasible headland turn manoeuvres," *Biosystems Engineering*, vol. 116(4), pp. 399-409, 2013.
- [11] M. Brezak, I. Petrovic, "Real-time approximation of clothoids with bounded error for path planning applications," *IEEE Transactions on Robotics*, vol. 30(2), pp. 507-515, 2013.
- [12] H. H. Triharminto, T. B. Adji, and N. A. Setiawan, "3D Dynamic UAV Path Planning for Interception of Moving Target in Cluttered Environment," *International Journal of Applied Mathematic and Statistics*, vol. 10(40), pp. 154-163, 2013.
- [13] R. Siegwart and I. R. Nourbakhsh, *Introduction to Autonomous Mobile Robots*, MIT Press, 2004.
- [14] L. Yin, Y. Yin, and C. J. Lin, "A new potential field method for mobile robot path planning in the dynamic environments," *Asian Journal of Control*, vol. 11(2), pp. 214-225, March 2009.
- [15] A. Sgorbissa and R. Zaccaria, "Planning and obstacle avoidance in mobile robotics," *Robotics and Autonomous System*, vol. 60(4), pp. 628-638, 2012.
- [16] P. Bhattacharya and M. L. Gavrilova, "Roadmap-Based Path Planning Using the Voronoi Diagram for a Clearance-Based Shortest Path," *IEEE Robotics and Automation Magazine*, pp. 58-66, 2008.
- [17] J. Guo, Y. Gao, and G. Cui, "Path Planning of Mobile Robot Based on Improved Potential Field," *Information Technology Journal*, vol. 12(11), pp. 2188-2194, 2013.
- [18] S. Hassan and J. Yoon, "Haptic assisted aircraft optimal assembly path planning scheme based on swarming and artificial potential field approach," *Advances in Engineering Software*, vol. 69, pp. 18-25, 2014.
- [19] O. Montiel, U. Orozco-Rosas, and R. Sepveda, "Path planning for mobile robots using Bacterial Potential Field for avoiding static and dynamic obstacles," *Expert Systems with Applications*, vol. 42(12), pp. 5177-5191, 2015.
- [20] Q. Zhang, D. Chen, and T. Chen, "An Obstacle Avoidance Method of Soccer Robot Based on Evolutionary Artificial Potential Field," *International Conference on Future Energy, Environment, and Materials, Energy Procedia*, vol. 16, pp. 1792-1798, 2012.
- [21] W. Liao and Z. Li, "Soccer robot path planning based on genetic potential field method," *Journal of Jimei University*, vol. 14(2), pp. 179-184, 2009.
- [22] L. Tang, S. Dian, G. Gu, K. Zhou, S. Wang, X. Feng, "A novel potential field method for obstacle avoidance and path planning of mobile robot," *IEEE International Conference on Computer Science and Information Technology (ICCSIT)*, vol. 9, pp. 633-637, 2010.
- [23] M. Kalavsky and Z. Ferkova, "Harmonic Potential Field Method for Path Planning of Mobile Robot," *International Virtual Conference (ICTIC 2012)*, vol. 1, pp. 41-46, 2012.
- [24] A. A. Masoud, "A harmonic potential field approach for joint planning and control of a rigid, separable nonholonomic, mobile robot," *Robotics and Autonomous Systems*, vol. 61, pp. 593-615, 2013.
- [25] H. J. S. Feder and J. J. E. Slotine, "Real-Time Path Planning Using Harmonic Potentials In Dynamic Environments," *IEEE International Conference on Robotics and Automation*, pp. 874-881, 1997.
- [26] F. Li, Y. Tan, Y. Wang, G. Ge, "Mobile Robots Path Planning Based on Evolutionary Artificial Potential Fields Approach," *Proceedings of the 2nd International Conference on Computer Science and Electronics Engineering (ICCSEE 2013)*, pp. 1314-1317, 2013.
- [27] J. Lee, Y. Nam, S. Hong, W. Cho, "New potential functions with random force algorithms using potential field method," *Journal of Intelligent Robotic System*, vol. 66(3), pp. 303-319, 2012.
- [28] X. Wang and Y. Ju, "An Application of Stream Function Method in Local Route Planning for UUV's", *International Industrial Informatics and Computer Engineering Conference (IIICEC 2015)*.
- [29] W. Honglun, L. Wentao, Y. Peng, L. Xiao, L. Chang, "Three-dimensional path planning for unmanned aerial vehicle based on interfered fluid dynamical system," *Chinese Journal of Aeronautics*, vol. 28(1), pp. 229-239, 2015.
- [30] J. Sfeir, M. Saad, H. Saliha-Hassane, "An Improved Artificial Potential Field Approach to Real-Time Mobile Robot Path Planning in an Unknown Environment," *IEEE International Symposium on Robotic and Sensors Environments (ROSE)*, pp. 208-213, 2011.
- [31] M. Wang, Z. Su, D. Tu, X. Lu, "A Hybrid Algorithm Based on Artificial Potential Field and BUG for Path Planning of Mobile Robot," *2nd International Conference on Measurement, Information and Control*, pp. 1393-1398, 2013.

- [32] J. W. Choi, "A potential field and bug compound navigation algorithm for nonholonomic wheeled robots," *Innovative Engineering Systems (ICIES)*, First International Conference on, vol.7-9, pp.166-171, 2012.
- [33] A. A. Ahmed, T. Y. Abdalla, and A. A. Abed, "Path Planning of Mobile Robot by using Modified Optimized Potential Field Method," *International Journal of Computer Applications*, vol. 113(4), pp. 0975-8887, March 2015.